Expanded View Figures

Figure EV1. RADX expression, localization, and alignment with RPA1.

A Alignment of the regions comprising OB-folds 2 and 3 in human RADX and the ssDNA-binding DBD-A and DBD-B OB-folds in human RPA1 (Fig 1A). The positions of the K263 and E277 residues in RPA1 and the corresponding K304 and E327 residues in RADX, mutated in RADX *OB, are indicated by asterisks.

B Immunoblot analysis of RADX expression in the indicated human cell lines.

C qPCR analysis of *RADX* mRNA levels in indicated cell lines relative to HCT116 WT cells. Primers to *ubiquitin* were used as a control for normalization (mean ± SEM; $n = 3$ independent experiments).

D U2OS cells were synchronized in early S phase by double thymidine block, released into fresh medium for the indicated times, and analyzed by immunoblotting with indicated antibodies.

E U2OS cell lines stably reconstituted with GFP-RADX alleles were treated or not with doxycycline (DOX) to induce the transgenes and immunoblotted with GFP and tubulin antibodies.

F Cells in (E) were fixed with paraformaldehyde and analyzed by microscopy to visualize GFP-RADX localization. Scale bar, 10 μm.

G Quantification of PLAs (Fig 1G) in BrdU-labeled U2OS and U2OS/GFP-RADX cell lines using GFP and BrdU antibodies under native conditions ($n \geq 3{,}000$ cells per condition; data from a representative experiment are shown).

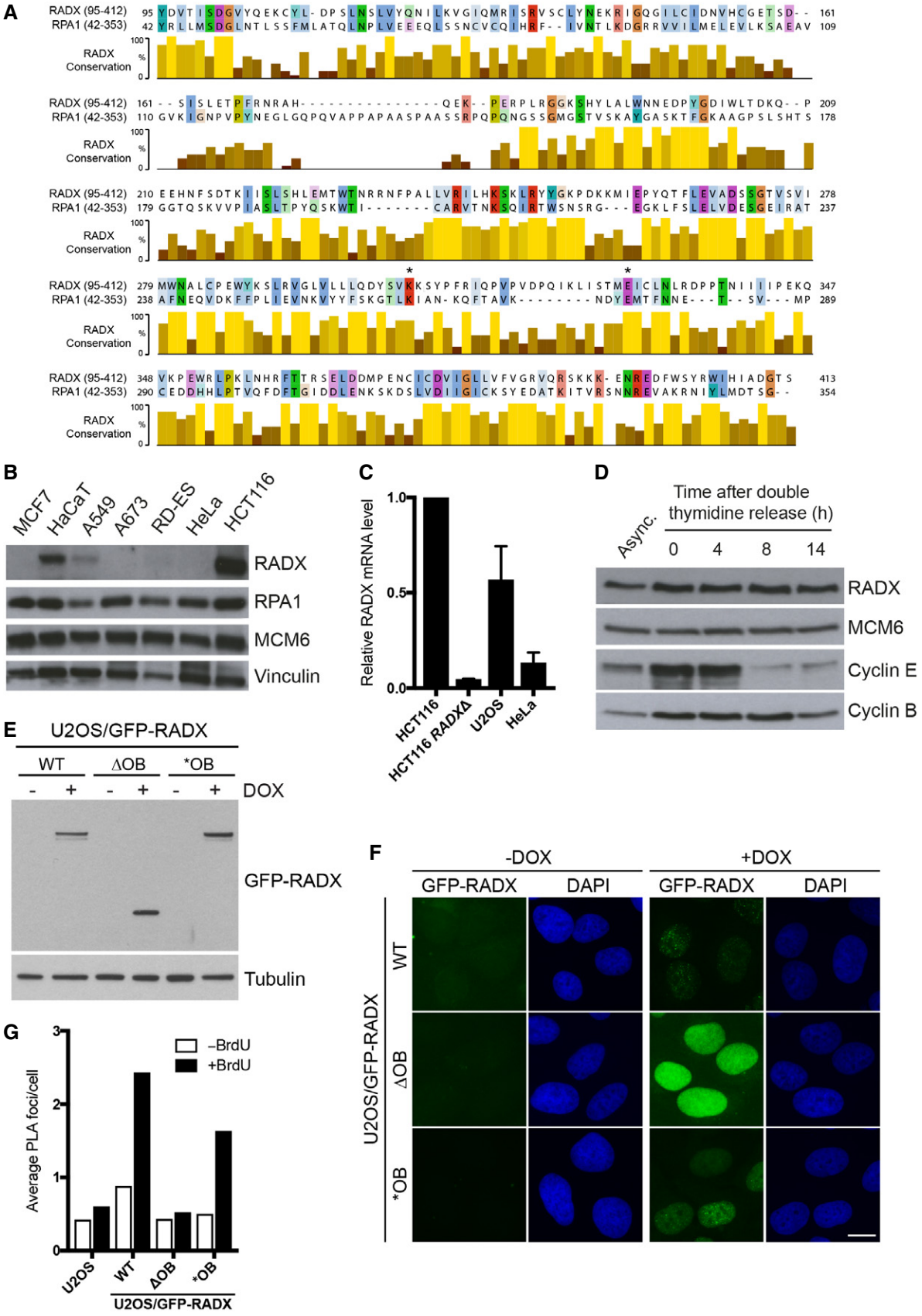
A
RADX (95-412)
RPA1 (42-353)
RADX Conservation
B
MCF7
HaCaT
A549
A673
RD-ES
HeLa
HCT116
RADX
RPA1
MCM6
Vinculin
C
Relative RADX mRNA level
HCT116
HCT116 RADXΔ
U2OS
HeLa
D
Time after double thymidine release (h)
Async.
0
4
8
14
RADX
MCM6
Cyclin E
Cyclin B
E
U2OS/GFP-RADX
WT
ΔOB
*OB
DOX
GFP-RADX
Tubulin
F
-DOX
+DOX
GFP-RADX
DAPI
U2OS/GFP-RADX
G
Average PLA foci/cell
–BrdU
+BrdU
U2OS
WT
ΔOB
*OB
U2OS/GFP-RADX

Figure EV1.

Figure EV2. RADX recruitment to replication stress sites.

A U2OS cells labeled with BrdU and treated with HU in the presence or absence of ATR inhibitor (ATRi) were fixed and immunostained under native conditions. Representative images are shown.

B U2OS/GFP-RADX cell lines treated with doxycycline to induce the transgenes were fixed with methanol/acetone and immunostained with PCNA antibody.

C As in (B), except cells were pre-extracted prior to fixation with paraformaldehyde and immunostained with RPA1 antibody.

D Quantification of PLAs (Fig 2E) with GFP and RPA2 antibodies in U2OS and U2OS/GFP-RADX cell lines labeled with EdU for 30 min and subsequently left untreated or exposed to HU or CPT for 4 h ($n \geq 3{,}000$ cells per condition; data from a representative experiment are shown).

Data information: All scale bars, 10 μm.

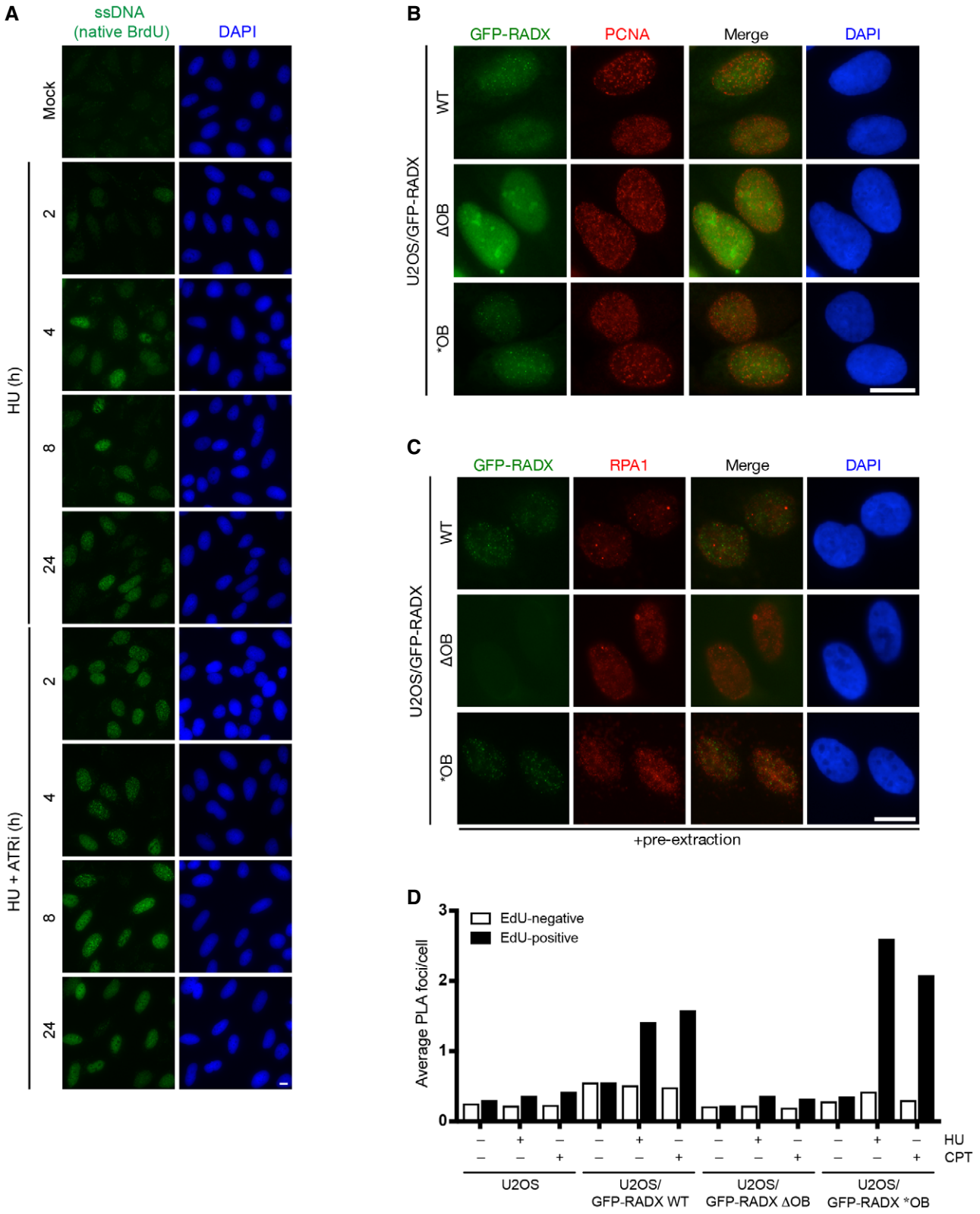

Figure EV2.

Figure EV3. Impact of RADX loss on cell cycle distribution, checkpoint signaling, and replication fork integrity.

A Quantitative image analysis of asynchronously growing HCT116 WT cells transfected with indicated RADX siRNAs (left) and HCT116 *RADX* knockout cell lines (*RADX*Δ) (right) labeled with EdU and stained with DAPI ($n \geq 3{,}000$ cells per condition). Proportion of cells in different cell cycle phases is indicated.

B HCT116 WT or *RADX*Δ cells were treated with HU or CPT for the indicated times, collected, and immunoblotted with indicated antibodies.

C U2OS cells transfected with indicated siRNAs were labeled with consecutive pulses of CldU and IdU as shown in Fig 3B. Replication fork speeds were calculated as length of labeled track divided by pulse time (bars, mean; $n = 200$ fibers, pooled from two independent experiments, per condition).

D Fork symmetry was calculated as the percentage of shorter divided by longer tracks from (C). Concordance is 100%, representing fully bidirectional replication and equal rates of elongation for both daughter forks (bars, mean; $n = 50$ bidirectional forks, pooled from two independent experiments, per condition).

E Proportion of new origins in U2OS cells treated as in (C) was determined (bars, mean; 20 fields of view quantified per condition; $n = 2$ independent experiments).

F HeLa cells transfected with control (CTRL) or RADX siRNA were labeled with consecutive pulses of CldU and IdU as shown in Fig 3B. Replication fork speeds were calculated as length of labeled track divided by pulse time (bars, mean; $n = 400$ fibers, pooled from two independent experiments, per condition).

G U2OS cells transfected with indicated siRNAs were labeled with CldU, then incubated with HU, washed, and labeled with IdU as shown in Fig 3G. The proportion of new origins was determined (bars, mean; 20 fields of view quantified per condition; $n = 2$ independent experiments).

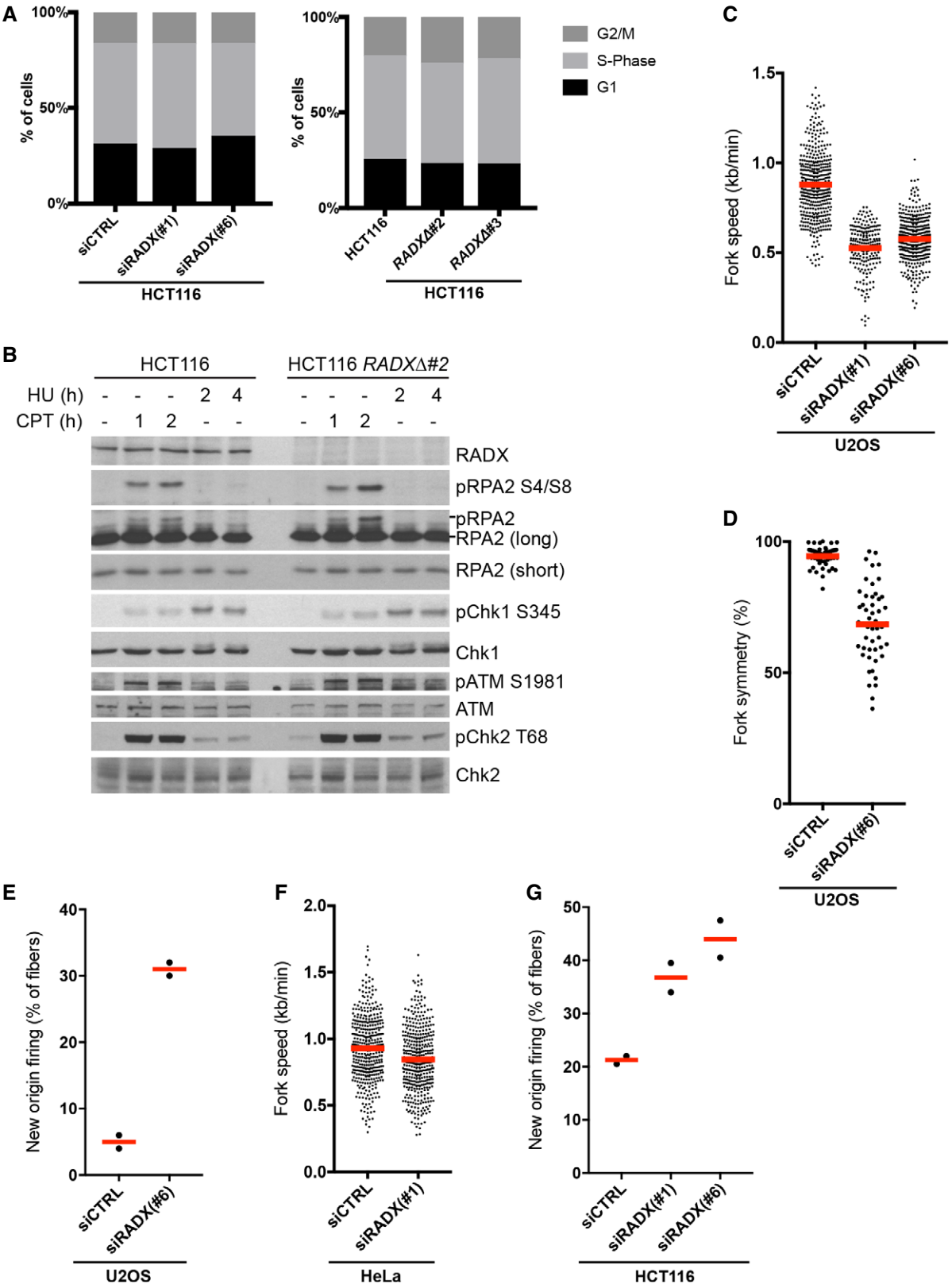
A
100%
50%
0%
% of cells
siCTRL
siRADX(#1)
siRADX(#6)
HCT116
HCT116
RADXΔ#2
RADXΔ#3
HCT116
G2/M
S-Phase
G1
B
HCT116
HCT116 RADXΔ#2
HU (h) - - - 2 4 - - - 2 4
CPT (h) - 1 2 - - - 1 2 - -
RADX
pRPA2 S4/S8
pRPA2
RPA2 (long)
RPA2 (short)
pChk1 S345
Chk1
pATM S1981
ATM
pChk2 T68
Chk2
C
Fork speed (kb/min)
1.5
1.0
0.5
0.0
siCTRL
siRADX(#1)
siRADX(#6)
U2OS
D
Fork symmetry (%)
100
50
0
siCTRL
siRADX(#6)
U2OS
E
New origin firing (% of fibers)
40
30
20
10
0
siCTRL
siRADX(#6)
U2OS
F
Fork speed (kb/min)
2.0
1.5
1.0
0.5
0.0
siCTRL
siRADX(#1)
HeLa
G
New origin firing (% of fibers)
50
40
30
20
10
0
siCTRL
siRADX(#1)
siRADX(#6)
HCT116

Figure EV3.

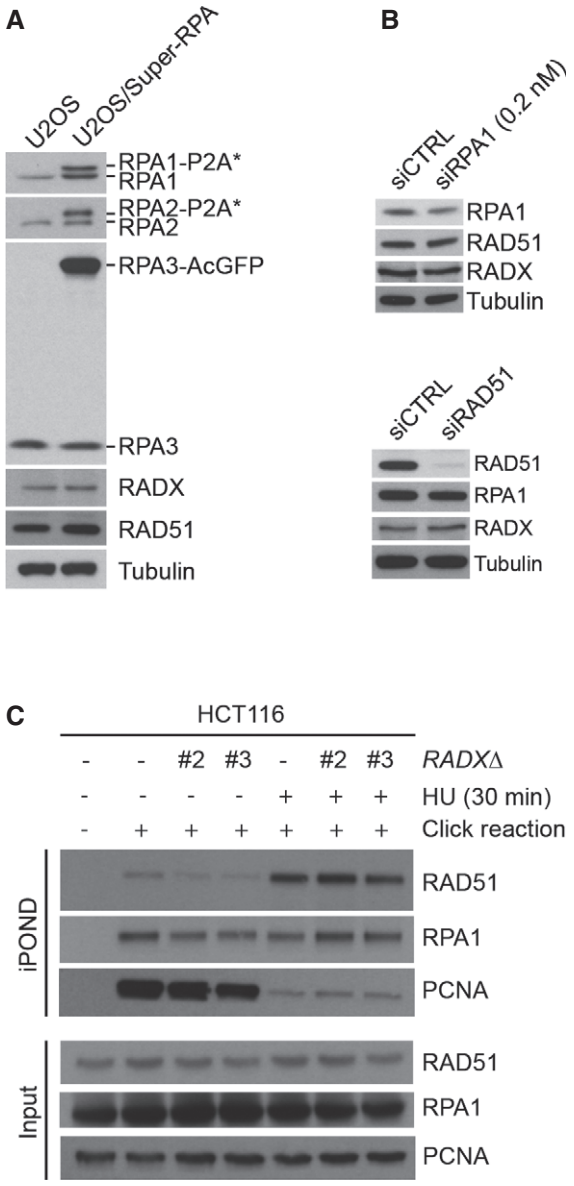

Figure EV4. RPA and RAD51 expression levels and association with replication forks under different experimental conditions.

A Immunoblot analysis of total extracts of U2OS/Super-RPA cells, using indicated antibodies. P2A, 2A peptide.

B Immunoblot analysis of RPA and RAD51 siRNA knockdown efficiency.

C Immunoblot analysis of levels of RAD51, RPA1, and PCNA associated with replication forks isolated by iPOND and in total cell extracts in HCT116 WT and *RADX*Δ cell lines.

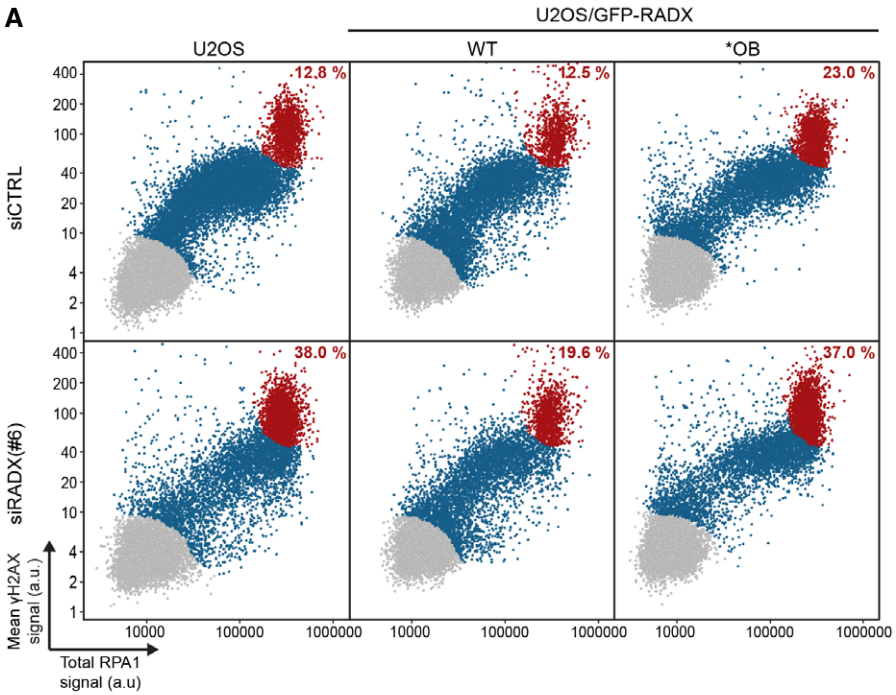

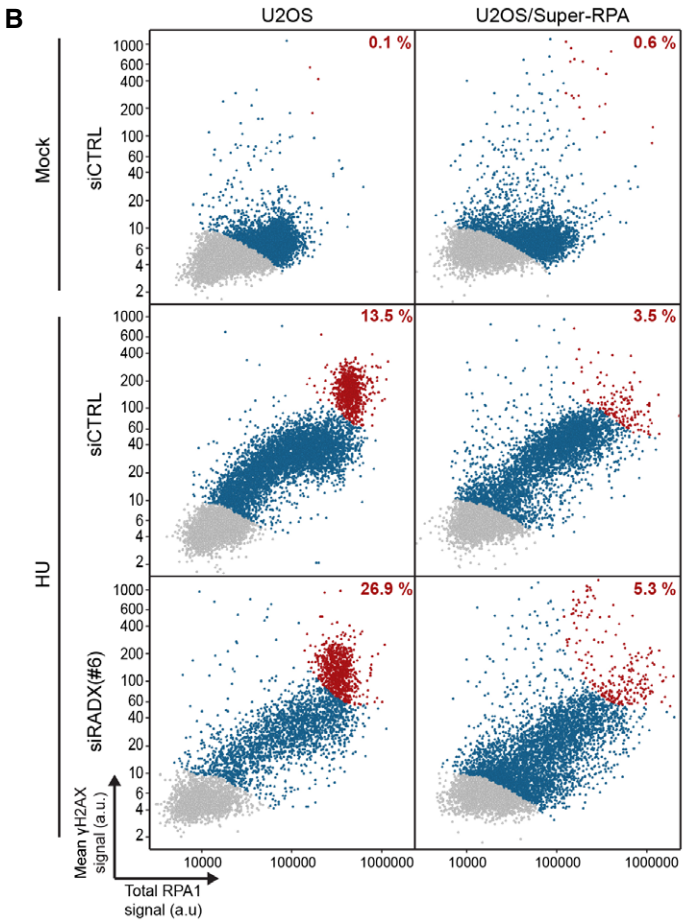

Figure EV5. Impact of altered RADX functionality on HU-induced replication catastrophe.

A U2OS or derivative U2OS/GFP-RADX cell lines transfected with indicated siRNAs and exposed to HU for 4 h were co-immunostained with RPA1 and γ-H2AX antibodies and subjected to quantitative image analysis of total RPA1 and mean γ-H2AX signal intensities in individual cells (each representing a single dot). Cells displaying maximal RPA chromatin loading accompanied by extensive DNA breakage (characterized by H2AX hyperphosphorylation) reflecting irreversible global replication catastrophe are indicated in red. Cells in blue show RPA1 and/or γ-H2AX signals above background levels. Proportion of cells showing replication catastrophe among all cells displaying RPA1 and/or γ-H2AX signals above background levels (blue and red) is indicated ($n \geq 3{,}000$ cells per condition; data from a representative experiment are shown). See also Fig 5D.

B As in (A), but using U2OS or U2OS/Super-RPA cells exposed or not to HU. Proportion of cells displaying replication catastrophe is indicated ($n \geq 3{,}000$ cells per condition; data from a representative experiment are shown). See also Fig 5E.